Evidence for changes in stratospheric transport and mixing over the past three decades based on multiple data sets and tropical leaky pipe analysis

Evidence for changes in stratospheric transport and mixing over the past three decades based on multiple data sets and tropical leaky pipe analysis

Eric A. Ray,[1,2] Fred L. Moore,[1,2] Karen H. Rosenlof,[1] Sean M. Davis,[1,2] Harald Boenisch,[3] Olaf Morgenstern,[4] Dan Smale,[4] Eugene Rozanov,[5,6] Michaela Hegglin,[7] Gianni Pitari,[8] Eva Mancini,[8] Peter Braesicke,[9] Neal Butchart,[10] Steven Hardiman,[10] Feng Li,[11] Kiyotaka Shibata,[12] and David A. Plummer[13]

Received 16 March 2010; revised 6 July 2010; accepted 14 July 2010; published 6 November 2010.

[1] Variability in the strength of the stratospheric Lagrangian mean meridional or Brewer-Dobson circulation and horizontal mixing into the tropics over the past three decades are examined using observations of stratospheric mean age of air and ozone. We use a simple representation of the stratosphere, the tropical leaky pipe (TLP) model, guided by mean meridional circulation and horizontal mixing changes in several reanalyses data sets and chemistry climate model (CCM) simulations, to help elucidate reasons for the observed changes in stratospheric mean age and ozone. We find that the TLP model is able to accurately simulate multiyear variability in ozone following recent major volcanic eruptions and the early 2000s sea surface temperature changes, as well as the lasting impact on mean age of relatively short-term circulation perturbations. We also find that the best quantitative agreement with the observed mean age and ozone trends over the past three decades is found assuming a small strengthening of the mean circulation in the lower stratosphere, a moderate weakening of the mean circulation in the middle and upper stratosphere, and a moderate increase in the horizontal mixing into the tropics. The mean age trends are strongly sensitive to trends in the horizontal mixing into the tropics, and the uncertainty in the mixing trends causes uncertainty in the mean circulation trends. Comparisons of the mean circulation and mixing changes suggested by the measurements with those from a recent suite of CCM runs reveal significant differences that may have important implications on the accurate simulation of future stratospheric climate.

Citation: Ray, E. A., et al. (2010), Evidence for changes in stratospheric transport and mixing over the past three decades based on multiple data sets and tropical leaky pipe analysis, *J. Geophys. Res.*, *115*, D21304, doi:10.1029/2010JD014206.

[1]Chemical Sciences Division, Earth Systems Research Laboratory, NOAA, Boulder, Colorado, USA.
[2]Cooperative Institute for Research in Environmental Sciences, University of Colorado, Boulder, Colorado, USA.
[3]Institute for Atmospheric and Environmental Sciences, Goethe Universität Frankfurt, Frankfurt, Germany.
[4]National Institute of Water and Atmospheric Research Ltd., Omakau, New Zealand.
[5]Physical-Meteorological Observatory/World Radiation Centre, Davos, Switzerland.
[6]Swiss Federal Institute of Technology, Zurich, Switzerland.
[7]Department of Physics, University of Toronto, Toronto, Canada.
[8]University of L'Aquila, L'Aquila, Italy.
[9]National Centre for Atmospheric Science Climate-Chemistry, Centre for Atmospheric Science, University of Cambridge, Cambridge, UK.
[10]Met Office Hadley Centre, Exeter, UK.
[11]Goddard Earth Sciences and Technology Center, University of Maryland Baltimore County, Baltimore, Maryland, USA.
[12]Meteorological Research Institute, Ibaraki, Japan.
[13]Canadian Centre for Climate Modelling and Analysis, Environment Canada, Québec, Canada.

0148-0227/10/2010JD014206

1. Introduction

[2] Current coupled chemistry climate model (CCM) simulations consistently suggest that the strength of the stratospheric Lagrangian mean meridional or Brewer-Dobson circulation has increased in recent decades and will continue to increase in response to future climate change scenarios [e.g., *Butchart et al.*, 2006; *Li et al.*, 2008; *Garcia and Randel*, 2008; *McLandress and Shepherd*, 2009]. This simulated strengthening of the Brewer-Dobson circulation is partially due to the changes in the vertical temperature gradient between the troposphere and stratosphere with the troposphere warming and the stratosphere cooling, an important "fingerprint" of climate change [e.g., *Shine et al.*, 2003; *Shepherd and Jonsson*, 2008]. A warming troposphere and cooling stratosphere causes the subtropical jet streams to strengthen, and this in turn affects the propagation and dissipation of waves in the stratosphere [e.g., *Butchart et al.*, 2010]. These changes in wave propagation and dissipation as well as possible increases in tropospheric wave activity are the primary drivers of the simulated strengthening

of the Brewer-Dobson circulation [e.g., *McLandress and Shepherd*, 2009; *Butchart et al.*, 2010].

[3] However, exactly how the Brewer-Dobson circulation has actually changed over recent decades is somewhat uncertain due to a lack of sufficient observations. The strength of the mean meridional circulation is not a directly measureable quantity, so inferences in regards to temporal variations have to be made based on measurements of chemical species and temperatures. The best available observational evidence for changes in the Brewer-Dobson circulation in the last three decades has been largely confined to the lower stratosphere. This observational evidence primarily comes from temperature and ozone measurements, especially the microwave sounding unit channel 4 (MSU4) and the advanced microwave sounding unit channel 9 (AMSU9) temperatures (collectively called TLS for temperature lower stratosphere) [*Mears and Wentz*, 2009] and total ozone mapping spectrometer/solar backscatter ultraviolet (TOMS/SBUV) total ozone [*Stolarski et al.*, 2006]. TLS temperatures are weighted over a broad region of the lower stratosphere, with a peak at ~70 hPa. Trends of the TLS temperatures are mostly negative in the tropics and positive in the extratropical winters [e.g., *Randel et al.*, 2009]. This out-of-phase relationship is suggestive of a change in circulation strength that is most noticeable in the winter seasons of each hemisphere. Total ozone, although a measure of ozone throughout the entire atmosphere, has been shown to have variability largely weighted by ozone changes in the lower stratosphere [e.g., *Randel and Cobb*, 1994; *Thompson and Solomon*, 2009]. Trends of total ozone are negative throughout the stratosphere, with some part of this trend due to polar photochemical ozone depletion. Total ozone variability is notoriously difficult to interpret due to the large range of photochemical lifetimes of ozone in the stratosphere. Many studies have interpreted various aspects of the time series of total ozone using regression and model analysis [e.g., *Marsh and Garcia*, 2007; *Fleming et al.*, 2007; *Stolarski et al.*, 2006; *Lee and Smith*, 2003; *Hadjinicolaou et al.*, 2002]. But there is still not a consensus on what part of the variability is due to long-term changes in the Brewer-Dobson circulation. An empirical study by *Hood and Soukharev* [2005], although focused only on the Northern Hemisphere (NH) midlatitudes, does suggest that up to roughly 25% of the negative total ozone trend in the NH midlatitudes is due to long-term changes in the Brewer-Dobson circulation. This contribution to the negative total ozone trend in midlatitudes is due to a decrease in Eliassen-Palm (EP) flux and thus an implied slowing of the Brewer-Dobson circulation and less downward advection of high-ozone mixing ratios to the lower stratosphere. A recent study by *Thompson and Solomon* [2009] made use of coincident variability in TOMS/SBUV total ozone and MSU4 temperatures to show that the residual temperature variability had cooling in the tropics and warming in the high latitudes, suggestive of a strengthening circulation in the lower stratosphere. In the tropical tropopause region, observed decreases in ozone mixing ratios [*Randel and Wu*, 2007] and cooling temperatures [*Seidel et al.*, 2001] are also consistent with an increasing tropical upwelling in the Brewer-Dobson circulation. Most of this observational evidence is in support of an increase in the strength of the Brewer-Dobson circulation in the lower stratosphere, but there is no similar observational evidence in regards to the strength of the circulation in the middle and upper stratosphere.

[4] Along with the simulated change in the Brewer-Dobson circulation by CCMs is a simulated decrease in stratospheric mean age of air, which is an indicator of how long air has resided in the stratosphere [*Austin and Li*, 2006; *Garcia et al.*, 2007; *Lamarque et al.*, 2008; *Oman et al.*, 2009]. The negative modeled mean age trend over the past three decades is present throughout the depth of the stratosphere due to the close connection between mean circulation strength and mean age of air in CCMs [e.g., *Austin and Li*, 2006]. The mean age of air is dependent on both the strength of the Brewer-Dobson circulation as well as mixing between the extratropics and tropics or the tropical recirculation of air [*Waugh and Hall*, 2002]. Mixing into the tropics from the midlatitudes has been shown to be important in determining tropical tracer mixing ratios such as water vapor [e.g., *Mote et al.*, 1998], long-lived photolytic tracers [*Volk et al.*, 1996], and ozone [e.g., *Konopka et al.*, 2009]. But the sensitivity of mixing between the midlatitudes and tropics on the mean age in models has not been studied extensively. *Bacmeister et al.* [1998] used a zonally averaged 2-D model to quantify the effect of mixing on mean age. They showed that mean ages were 1–2 years younger throughout most of the stratosphere when mixing was not present. They also showed that mean age values without including mixing were insensitive to changes in planetary wave forcing, whereas mean age with mixing increases in the presence of greater planetary wave forcing. A recent study by *Strahan et al.* [2009] demonstrates the importance of tropical recirculation to the simulation of polar chemical composition. The study compared two chemical transport models (CTM) to observationally derived age characteristics and polar trace gas distributions. Even though both the CTMs had reasonable mean vertical transport rates in the tropics, there was too little mixing from the midlatitudes into the tropics. This insufficient mixing was shown to cause polar chemical composition to be much different from that observed. The implication is that inadequate tropical recirculation has a global impact on the distribution of chemical species. Since mean age reveals information about two major transport characteristics of the stratosphere, it is clearly an important quantity to simulate accurately.

[5] Until recently, a long-term, observationally derived mean age data set had not been available. That changed with the publication by *Engel et al.* [2009] of a data set of observationally derived mean age of air over the last 30 years. These mean ages from *Engel et al.* [2009] were derived from SF_6 and CO_2 balloon measurements in the Northern Hemisphere midlatitude stratosphere in the 30–5 hPa region. This is higher in the stratosphere than the peak weighting altitudes of the ozone and temperature satellite observations mentioned above. But since the mean age is sensitive to circulation and mixing changes below the level considered, this mean age data set provides information about circulation and mixing changes throughout the depth of the stratosphere. *Engel et al.* [2009] calculated this mean age data set to have a positive trend of 0.24 ± 0.22 years/decade over the last 30 years. Error analysis on the trend showed that it is not statistically significant at the 90% confidence level, thus *Engel et al.* [2009] concluded that the mean age is essentially unchanged over the

period of observations. *Waugh* [2009] calculated mean age trends of −0.05 to −0.20 years/decade from four CCMs over the same time period and averaged over the same region of the stratosphere as the *Engel et al.* [2009] observations. Although the observed mean age trends may not be statistically different at a high confidence level from some of the model trends, the different sign of the observed and modeled mean age trends points to a possible deficiency in modeled circulation and/or mixing trends.

[6] In this study, we use a simple representation of the stratosphere, the tropical leaky pipe (TLP) model [*Neu and Plumb*, 1999], to show possible mean circulation and horizontal mixing changes that help explain the observed changes in mean age estimates and TOMS/SBUV total ozone. We use the TLP model since, although it is relatively simple, it does a reasonable job of representing mean age in the stratosphere [e.g., *Hall and Waugh*, 2000] and includes transport by the mean circulation as well as horizontal mixing between the midlatitudes and tropics. To help guide the TLP model simulations, we use mean circulation and mixing variability in several reanalysis data sets and we compare the output to that from an average of a number of CCMs. There are a number of interesting results from this analysis, including the simulation of ozone and mean age variability following transient events such as volcanoes and tropical SST changes, and the simulation of a positive mean age trend in the midlatitude midstratosphere even in the presence of a strengthening Brewer-Dobson circulation in the lower stratosphere. Perhaps the most significant result is the clear demonstration of the importance of changes in mixing between the midlatitudes and tropics in the determination of mean age variability throughout the stratosphere and how this may explain the discrepancy between the observed and simulated mean age trends.

2. Data

[7] The primary long-term stratospheric observations we use in the analysis are midlatitude stratospheric mean age of air derived from SF_6 and CO_2 balloon-borne measurements [*Engel et al.*, 2009] and total column ozone measurements from the merged TOMS/SBUV data set [*Stolarski et al.*, 2006; *Stolarski and Frith*, 2006]. We also use Stratospheric Aerosol and Gas Experiment (SAGE) II ozone measurements [*McCormick et al.*, 1989] to initialize the TLP model and the *Randel and Wu* [2007] ozone profile data set derived largely from SAGE I and II measurements to compare to some of the TLP model results.

[8] The stratospheric mean age of air data set spans the time period from 1975 to 2005 with a total of 33 calculated mean age values from 27 individual balloon flights [*Engel et al.*, 2009]. Only flights in the 32°–51°N latitude range were included in the data set, and the mean ages were averaged from 30 to between 10 and 5 hPa, depending on the maximum level attained by each balloon. Mean age of air is roughly constant in the midlatitude stratosphere above 30 hPa [*Engel et al.*, 2009], so the different range of maximum levels above this should have little effect on the calculated mean ages. Uncertainty estimates by *Engel et al.* [2009] range from 0.78 to 1.45 years for the mean ages that range from 3.8 to 5.8 years. The relatively large uncertainties led to the result in *Engel et al.* [2009] that their calculated positive linear trend of 0.24 years/decade was not statistically significant at the 90% confidence level.

[9] The total uncertainty estimates are the sum of eight different sources of potential error with one of the largest being the representativeness of an individual profile. The other sources of error are due to uncertainties in surface emission data, fit to the tropospheric growth rate, the parameterization of the age spectrum, absolute measurement scales, the seasonality of transport into the stratosphere, the spatial representativeness of the tropospheric source data, and the reproducibility of the measurements. This profile representativeness error is due to the fact that there is a latitudinal gradient in mean age [*Hall et al.*, 1999], and thus, a single profile location may not represent the average midlatitude mean age. We have attempted to correct for this representativeness error by removing the slope of mean age as a function of equivalent latitude. This slope was estimated to be 0.25 years/10° latitude, which is consistent with the slope of previous measurement-based mean ages in the 30°N–55°N latitude range [*Hall et al.*, 1999]. The equivalent latitudes of each measurement location were calculated using National Centers for Environmental Prediction (NCEP)/National Center for Atmospheric Research (NCAR) Reanalysis output. With the mean age versus equivalent latitude slope removed, we conservatively reduced the mean age error by 0.15 years, which is half or less of the representativeness error values estimated by *Engel et al.* [2009]. The removal of this equivalent latitude variability does not affect the mean value of the trend.

[10] Total column ozone measurements from the merged total ozone mapping spectrometer/solar backscatter ultraviolet (TOMS/SBUV) data set [*Stolarski et al.*, 2006] are also used in this study. This data set combines most of the different TOMS and SBUV satellite measurements into one time series from 1979 to 2009 (http://code916.gsfc.nasa.gov/Data_services/merged). The *Randel and Wu* [2007] stratospheric ozone profile data set uses SAGE I and II as well as polar ozonesonde measurements merged into a monthly mean time series from 1979 to 2005. Trends from this data set are useful to compare in at least a qualitative sense to the ozone trend profiles obtained from the TLP model. However, since the *Randel and Wu* [2007] data set does not extend a full 30 years and it is not as well validated as the TOMS/SBUV total ozone, we chose to make detailed comparisons of the TLP model output to the TOMS/SBUV total ozone.

[11] For long-term meteorology of the stratosphere, we use three reanalyses: the Japanese 25 year Reanalysis Project (JRA-25) [*Onogi et al.*, 2007], the ECMWF Reanalysis (ERA-40) [*Uppala et al.*, 2005], and the NCEP/NCAR Reanalysis 1 (NCEP) [*Kalnay et al.*, 1996]. JRA-25 has higher resolution than either ERA-40 or NCEP, but we use all of them to help guide the inputs to the TLP model. JRA-25 and NCEP cover the period from 1979 to 2008, thereby effectively spanning the period of both the total ozone and mean age observations. ERA-40 covers the time period September 1957 to August 2002; NCEP starts in 1948. However, we only use output starting in 1979 when satellite temperatures were initially introduced for any trend analysis. We also use mean age of air and tropical upwelling output from the REF-B1 simulations of nine different chemistry climate models that participated in the Chemistry Climate

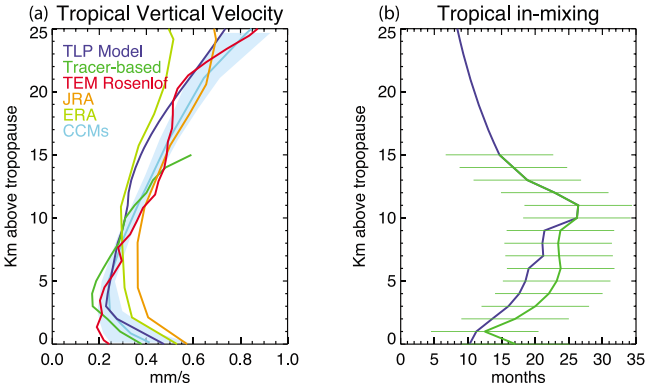

Figure 1. Profiles of (a) the tropical vertical velocity and (b) the midlatitude-to-tropics mixing time scale τ used in the TLP model. The TEM Rosenlof vertical velocities are described by *Rosenlof* [1995], and the JRA and ERA vertical velocities are from a TEM calculation of the residual mean circulation using those reanalysis data sets. The CCM profile is an average of the nine models described in section 2, with the standard deviation at each level shown by the light blue–shaded region. The Rosenlof, JRA, ERA, and CCM vertical velocities are multiple year averages from 20°S to 20°N. The tracer-based vertical velocity and τ values come from *Volk et al.* [2000].

Model Validation 2 (CCMVal-2) activity [*Eyring et al.*, 2010]. The models included in this study were CMAM, GEOS CCM, MRI, Niwa-SOCOL, SOCOL, ULAQ, UMUKCA-METO, UMUKCA-UCAM, and WACCM (see *Eyring et al.* [2010] and *Morgenstern et al.* [2010] for model details). These models were selected due to the fact that all have both mean age and vertical velocities available in the CCMVal-2 data archive. The REF-B1 simulations covered the period from 1960 to 2006, and we only used model output after 1978 to calculate trends.

3. Tropical Leaky Pipe Model

[12] The TLP model was formulated by *Neu and Plumb* [1999] based on the original tropical pipe model of *Plumb* [1996]. The model is a set of three coupled 1-D equations, one for the tropics and one each for the northern and southern midlatitudes. The model is made "leaky" by including a term that allows mixing of air from the midlatitudes into the tropics to be consistent with observations of the tropical stratosphere [e.g., *Volk et al.*, 1996; *Mote et al.*, 1998]. The simple formulation of the TLP model is useful for examining large-scale variability in the stratosphere without the complexity of full 2-D and 3-D models and allows us to directly test the impact of assumed changes in tropical upwelling and mixing parameterizations on stratospheric mean age and ozone trends.

[13] The tropical and midlatitude continuity equations of the TLP model are given by

$$\frac{\partial q_T}{\partial t} + W_T \frac{\partial q_T}{\partial Z} = -\frac{1}{\tau}(q_T - q_M) + K_T e^{Z/H} \frac{\partial}{\partial Z}\left(e^{-Z/H}\frac{\partial q_T}{\partial Z}\right) + S_T, \quad (1)$$

$$\frac{\partial q_M}{\partial t} + W_M \frac{\partial q_M}{\partial Z} = \left(\lambda + \frac{\alpha}{\tau}\right)(q_T - q_M) - K_M e^{Z/H} \frac{\partial}{\partial Z} \cdot \left(e^{-Z/H}\frac{\partial q_M}{\partial Z}\right) + S_M, \quad (2)$$

where the subscripts T and M refer to the tropics and midlatitudes, respectively, q is a tracer mixing ratio, W is vertical velocity, K is the vertical diffusivity, H is a constant scale height (7 km), $\alpha \equiv M_T/(2M_M)$ is the ratio of tropical to midlatitude mass, $\lambda = -\alpha e^{Z/H}\frac{\partial}{\partial Z}(e^{-Z/H}W_T(Z))$ is the net tropical to midlatitude mass flux rate, τ is the time scale for tropical tracer values to relax to midlatitude values, and S is the tracer source/sink. We set the tropical barrier at 20° so that $\alpha \approx 0.5$ and use vertically constant values of $K_T = K_M = 0.1$ m^2/s consistent with observational studies [e.g., *Sparling et al.*, 1997; *Legras et al.*, 2003]. The tropical and midlatitude vertical velocities are related by α such that $W_M(Z) = -\alpha W_T(Z)$. The vertical coordinate Z is altitude above the tropopause, and the model was run with a vertical resolution of 1 km since higher vertical resolution did not affect the results.

[14] The vertical velocity W and the mixing time scale τ were constrained by observationally based estimates of these quantities. We used annually averaged transport vertical velocities from a Transformed Eulerian Mean (TEM) residual circulation calculation described by *Rosenlof* [1995] and a τ profile calculated from in situ photolytic tracer measurements [*Volk et al.*, 2000]. The observationally based and model-based tropical vertical velocity and τ profiles, all averaged over the tropics from 20°S to 20°N, and the profiles used in the TLP model are shown in Figure 1. The profiles used in the TLP model differ somewhat from the observationally and model-based profiles due to the need to have realistic profiles of ozone photochemical production and loss rates as described below. The reanalysis data sets do not necessarily accurately represent the stratospheric mean circulation [e.g., *Monge-Sanz et al.*, 2007], so we attempted to fit the TLP model upwelling most closely to the observationally based upwelling profiles. The model results discussed in this paper are robust to small changes in the initial vertical velocity and τ profiles.

[15] We performed simulations for two different types of tracers, an age tracer and an ozone-like tracer. For the age tracer, $S_T = S_M = 0$, while for the ozone tracer we used photochemical production and loss rates from a 2-D model [*Portmann et al.*, 1999] such that $S_T = P_T - L_T q_T$ and $S_M = P_M - L_M q_M$. A temporally linearly growing age tracer was initialized at $t = 0$ and $Z = 0$ in the tropics and the age tracer profiles in the tropics and midlatitudes were subsequently allowed to evolve to steady state. The only boundary condition used was at $Z = 0$ in the tropics, which is the only place air enters into the stratosphere in this model. At this location at each time step the age tracer was set to the value of the linearly growing age tracer so that mean age always equaled zero at $Z = 0$ in the tropics. Each simulation was run for 30 years before any perturbations in the circulation were applied to allow the mean age profiles to reach a steady state for at least 10 years. The ozone tracer profiles in the model were initialized using annually averaged tropical and midlatitude SAGE II measurements [*McCormick et al.*,

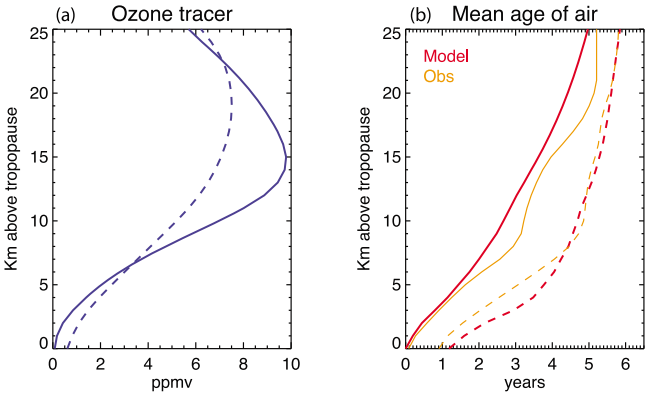

Figure 2. Profiles of (a) the steady state ozone and (b) mean age from the tropical pipe model. Solid lines are tropical, and dashed lines are midlatitudes. The ozone profiles are SAGE II annual averages in 20°S–20°N for the tropics and 30°–60°N for the midlatitudes. The mean age plot also includes profiles based on observations from *Engel et al.* [2009].

1989]. The model ozone profiles were identically matched to the SAGE II profiles by adjusting the vertical velocity and inmixing time scale τ so that the photochemical term in equations (1) and (2) exactly balanced the advection and diffusion terms and the photochemical production and loss rate profiles closely matched the 2-D model profiles. As shown in Figure 1, the adjustments made to W and τ were within the error estimates of the observationally based profiles. As with the age tracer, the only boundary condition applied was at $Z = 0$ in the tropics where the ozone was set equal to the SAGE II tropical tropopause value at each time step. No other boundary conditions are necessary in the simulations performed for this study, since the goal was to allow the tracers to freely evolve in response to perturbations in the mean circulation and mixing.

[16] The tropical and midlatitude steady state profiles of the mean age of air and ozone tracer are shown in Figure 2. The model mean age of air profiles very closely match the observed profiles from A. Engel et al. (personal communication) in both absolute values and shape. The current Engel et al. study is an extension of *Engel et al.* [2009] to include both the vertical and latitudinal distributions of observationally derived mean age of air. The sharp kink in the observed midlatitude mean age of air roughly 8 km above the tropopause is not reproduced by the model, but the model does show a change in vertical gradient between 8 and 10 km with a more gradual increase in mean age at higher altitudes. To compare the model output to the observed mean ages from *Engel et al.* [2009], we averaged the model output from 15 to 25 km above the tropopause.

4. Observed Mean Age of Air and Total Ozone

[17] The time series of observed midlatitude mean age of air with the equivalent latitude adjustment described in section 2 is shown in Figure 3. The slope of 0.24 ± 0.22 years/decade or 4.8% ± 4.5%/decade is the same as that calculated by *Engel et al.* [2009]. The uncertainty on the slope is mostly due to the uncertainties on the mean age estimates described in section 2. But the three low mean ages based on CO_2 measurements in 2001–2002 also make a significant contribution to the slope uncertainty and reduce the slope value. Two of the anomalously low CO_2 based mean ages have coincident SF_6 based mean ages that are over one year older and comparable to mean ages before and after this period. Since SF_6 has no significant change in growth rate during this period, there is no reason to suspect a problem in the SF_6 based mean ages. The reason for the low CO_2 based ages is uncertain but could be related to the SST-driven circulation changes that began in the year 2000 interacting with the seasonal cycle of CO_2 entering the stratosphere. Without these three points, the slope increases to 0.31 ± 0.22 years/decade, which is significant at the 90% confidence level. We chose to keep these three points in the time series since we have no conclusive reason to exclude them and thus use the lower value of the slope.

[18] It is interesting to note that some of the variability on time scales of 3–5 years, such as around 1985 and 1995, may be real and not due to errors in either the measurements or calculation of mean age (perhaps related to ENSO or other perturbations in the strength of the mean meridional circulation). In simulations of the TLP model (not shown), we found that several year increases in the middle and upper stratospheric mean circulation consistent with those seen in the JRA-25 residual circulation could explain some part of the decreases in observed mean age in the mid-1980s and 1990s.

[19] For the TOMS/SBUV total ozone, we use multiple linear regression to remove as much of the variability produced by known cycles and trends in order to attempt to isolate the part of the variability due to circulation changes. We use the 20°S–20°N average for the tropical time series and 30°–70° average in each hemisphere for the midlatitude time series and remove the seasonal cycle from each time series before performing the regression. We include in the regression two terms for the QBO (NCEP/NCAR Reanalysis tropical winds at 10 and 50 hPa), the solar cycle (10.7 μm radio flux), equivalent effective stratospheric chlorine (EESC) (from *Newman et al.* [2007], 2 year mean age time series in tropics and 5 year mean age time series in midlatitudes), stratospheric aerosol from volcanoes [*Deshler et al.*, 2006]

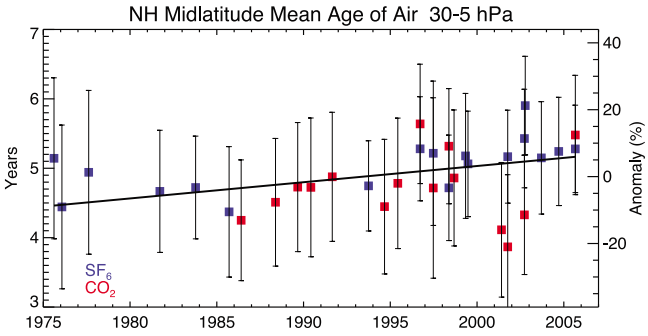

Figure 3. Time series of Northern Hemisphere midlatitude mean age of air calculated from balloon observations of SF_6 and CO_2 from *Engel et al.* [2009]. Variability as a function of equivalent latitude at each measurement location has been removed, and the error bars have been reduced slightly as a result. See text for details.

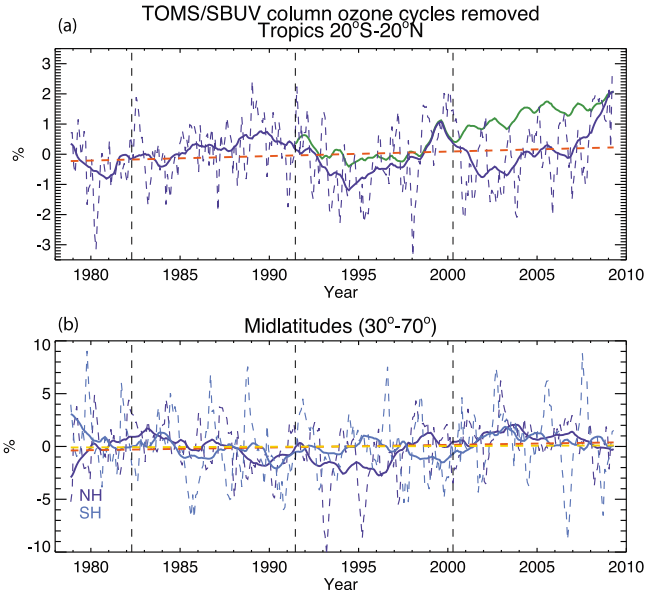

Figure 4. Time series of TOMS/SBUV total ozone in (a) the tropics and (b) midlatitudes with variability due to EESC, ENSO, QBO, the solar cycle, volcanoes, and the seasonal cycle removed. The solid lines have been smoothed with a 26 month boxcar average. The solid green line in Figure 4a represents the smoothed tropical total ozone time series with Pinatubo and post-year 2000 circulation related ozone variability calculated by the TLP model (Figures 5 and 6, see text for details) removed. Vertical dashed lines represent the eruptions of El Chichón and Mount Pinatubo and the year 2000 circulation changes. Linear fits are shown by the orange dashed lines for the tropics and NH midlatitudes and the yellow dashed line for the SH midlatitudes.

and ENSO (NOAA multivariate index lagged 6 months, only in the tropics [*Marsh and Garcia*, 2007]).

[20] Figure 4 shows the residual from the total ozone regression analysis with a smoothed version of each time series shown by the solid lines. The three vertical dashed lines in the panels represent the dates of the eruptions of El Chichón and Pinatubo and the previously noted tropical upwelling changes in the year 2000 [e.g., *Rosenlof and Reid*, 2008; *Randel et al.*, 2006]. The tropical residual total ozone time series clearly shows multiyear decreases following Pinatubo and the year 2000 and an overall positive trend. In the midlatitudes there is no significant trend in the residual time series and the variability associated with the volcanoes and year 2000 perturbations are weaker, particularly in the Southern Hemisphere (SH). In the Northern Hemisphere there is an ozone decrease following Pinatubo, and in both hemispheres there is an increase following the year 2000. We will show in the following section that the changes in midlatitude and tropical ozone following 2000 are consistent with an increased circulation in the lower stratosphere.

[21] A similar multiple regression analysis was performed on the *Randel and Wu* [2007] ozone profile data set with trends analyzed on the residual time series. The resulting trend profile in the tropics (not shown) has negative values peaking at −0.6%/decade in the lowest 5 km of the stratosphere and smaller positive values in the 5–10 km range above the tropopause. In the midlatitudes, the residual trends are 0.1%–0.2 %/decade in the lowest 5 km of the stratosphere and not significant above that. The rough shape of these profile trends will be used to compare to the TLP trend analysis.

5. TLP Model Simulations of Mean Age and Total Ozone

[22] The TLP model was used to simulate mean age and total ozone responses to photochemical, mean circulation and mixing perturbations caused by the eruptions of El Chichón and Pinatubo, the tropical sea surface temperature changes following the year 2000 and the possible long-term transport trends in the stratosphere. The volcano perturbation simulations were run primarily as a useful check that the TLP model can reproduce observed and previously modeled total ozone variability associated with the volcanoes with realistic inputs. The SST-related perturbations to the stratospheric circulation post-2000 clearly had an impact on the total ozone as seen in Figure 4 and thus provide another case to test the TLP model. We follow this analysis of the relatively short-term variability with analysis of the long-term trends in total ozone and mean age assumed to be due to mean circulation and mixing trends. The following sections describe each of the simulations in more detail.

5.1. Volcanic Perturbations

[23] The eruptions of El Chichón in 1982 and Mt. Pinatubo in 1991 injected large amounts of sulfur dioxide into the stratosphere and resulted in substantial impacts on total ozone for years following the eruptions. To simulate the impact of the aerosols on ozone and mean age with the TLP model, we used results of 2-D model calculations from *Tie et al.* [1994] and *Rosenfield et al.* [1997] of the perturbations in photochemical loss and mean vertical velocity due to the Pinatubo aerosol loading as a function of time, latitude, and altitude. The change in stratospheric aerosol loading caused a change in vertical velocity in response to local heating from absorption of both longwave and shortwave radiation [e.g., *Tie et al.*, 1994]. Figure 5a shows the time series of photochemical loss and vertical velocity inputs to the TLP model as well as the total ozone response in the midlatitudes and tropics. Figure 5b shows the vertical distribution of the photochemical loss in the midlatitudes and vertical velocity perturbations 6 months following the Pinatubo eruption. The perturbations following El Chichón have the same distributions as for Pinatubo but with the magnitude reduced by a factor of 2. This was done to approximate the reduced amount of sulfur dioxide injected by El Chichón into the stratosphere compared to Pinatubo and the reduced impact of sulfate aerosols on ozone photochemical loss in the 1980s when there was less chlorine in the stratosphere compared to the early 1990s [e.g., *Solomon et al.*, 1996].

[24] From Figure 5a, we can see that the midlatitude total ozone loss from the TLP model peaks roughly 1.5–2 years following each eruption and is twice as large following Pinatubo compared to El Chichón. The light blue lines following Pinatubo represent chemical ozone loss from a nudged CCM run from *Telford et al.* [2009]. The magnitude and timing of the ozone loss from the TLP model agrees well with the CCM results. This is an important test for the

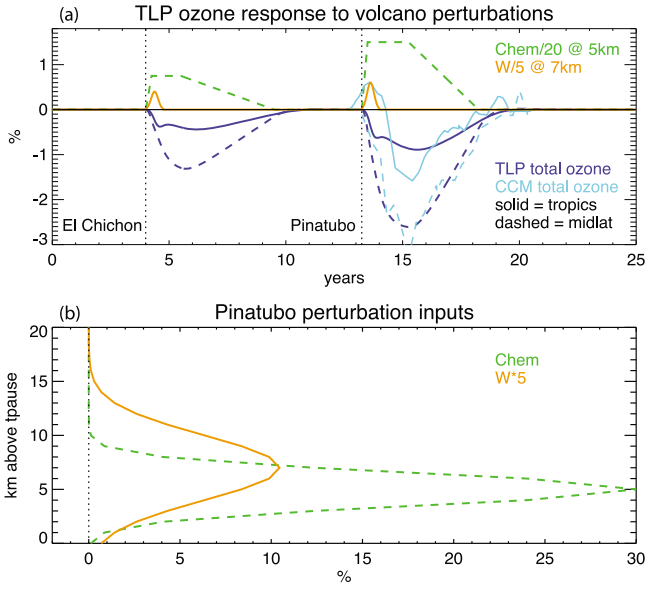

Figure 5. (a) TLP model total ozone response and input photochemical and circulation perturbations from the El Chichón and Pinatubo volcanoes plotted as a percentage difference from pre-Chichón values. The green dashed lines show the midlatitude photochemical perturbations scaled by a factor of 20 at 5 km above the tropopause and the solid orange lines are the vertical velocity perturbations scaled by a factor of 5 associated with aerosol heating at 7 km above the tropopause. The dark blue lines are the TLP model total ozone response in the tropics (solid) and midlatitudes (dashed). As a comparison the light blue lines show total ozone perturbations due to photochemistry following Pinatubo calculated by a CCM [*Telford et al.*, 2009]. (b) The vertical profiles of midlatitude photochemical and tropical vertical velocity perturbations 6 months following the Pinatubo eruption used as input to the TLP model. The vertical velocity perturbations are multiplied by 5 to show them more clearly.

transport in the TLP model since the tropical total ozone loss is almost entirely due to mixing of midlatitude air that has been depleted in ozone into the tropics where negligible chemical loss occurred. There are some differences in the shape of the tropical total ozone loss between the TLP and CCM, but the overall timing and magnitude of the peak loss and recovery is similar.

[25] To compare the total ozone perturbation following Pinatubo from the TLP model to that from the regression analysis described in section 4, the green line in Figure 4a shows the residual tropical total ozone time series with a regression that does not include volcanic aerosol, instead the TLP model Pinatubo perturbation from Figure 5a is removed. The green line after the year 2000 is due to the removal of SST-related variability and is described in the following section. Figure 4a shows that the TLP model tropical ozone perturbation following Pinatubo is significantly larger and longer lasting than that from the regression analysis with volcanic aerosol. There is still a slight decrease in tropical total ozone following Pinatubo even with the TLP model perturbation removed, but it is a significantly smaller decrease than the residual from the regression analysis. The reason for this discrepancy is not clear but may be due to the fact that the relationship between ozone and stratospheric aerosol is not described accurately by the linear regression. The midlatitude total ozone residual with the TLP model Pinatubo perturbation removed, rather than the regression including volcanic aerosol (not shown), is similar to that in the tropics in the NH, where the TLP model removes more of the decrease following Pinatubo than the regression. But for the SH, the TLP model perturbation adds a large increase in total ozone that is not present in the regression residual.

[26] The vertical velocity (w) perturbation shown by the orange lines in Figure 5 has only a small impact on the tropical total ozone within the first year following each eruption and no noticeable impact on the midlatitude total ozone. *Tie et al.* [1994] calculated the w perturbations from aerosol heating to peak a few months following Pinatubo with the largest increases of roughly 10% over the equator at 20 km altitude. The average perturbation over the tropics from 20°S to 20°N was certainly much smaller since the turnaround latitude where the w perturbation reversed sign was at roughly 20°. The w perturbations used in the TLP model volcano simulations maximize at a 2% increase. Larger increases were tried but they produced a very large negative peak in tropical total ozone within the first year following each volcano that is not seen in the observations (Figure 4). Thus, the 2% w increase is likely an upper limit on the average tropical perturbation due to volcano aerosol heating. Note also that the mean age from the model is not shown in Figure 5a due to the negligible response in the midstratospheric mean age from the volcano-induced transport perturbations.

5.2. SST Related Perturbations Post-2000

[27] The tropical lower stratospheric vertical velocity in the year 2000 increased by 15%–20% over the previous 5-year average, and this increase was sustained for a period of at least 5–6 years [*Rosenlof and Reid*, 2008]. The cause of the increase is not fully understood but may have been connected to a region of warmer than average tropical Pacific sea surface temperatures as suggested by *Rosenlof and Reid* [2008]. This circulation change caused large decreases in stratospheric water vapor and tropical ozone [*Solomon et al.*, 2010; *Rosenlof and Reid*, 2008; *Randel et al.*, 2006] and changes in stratospheric tracer correlations (H. Boenisch et al., A hint for a changing stratospheric circulation pattern after 2000, submitted to *Atmospheric Chemistry and Physics Discussions*, 2010). The dramatic change in the lower stratospheric circulation provides another perturbation case to be simulated by the TLP model.

[28] Figure 6 shows the w perturbations used as input into the model and the ozone and mean age responses. The shape and magnitude of the perturbations as a function of time are indicated by the orange line in Figure 6a. The characteristics of these perturbations were guided by calculations of the TEM residual vertical velocity [*Rosenlof and Reid*, 2008] and the observations of tropical total ozone, which suggests a reduction in the increased tropical upwelling back to pre-2000 values beginning roughly in 2006 or 2007 (shown in Figure 4a). The w perturbations peaked at the tropopause and were confined to the lowest 5 km of the stratosphere (Figure 6b). There were likely also changes in the mixing

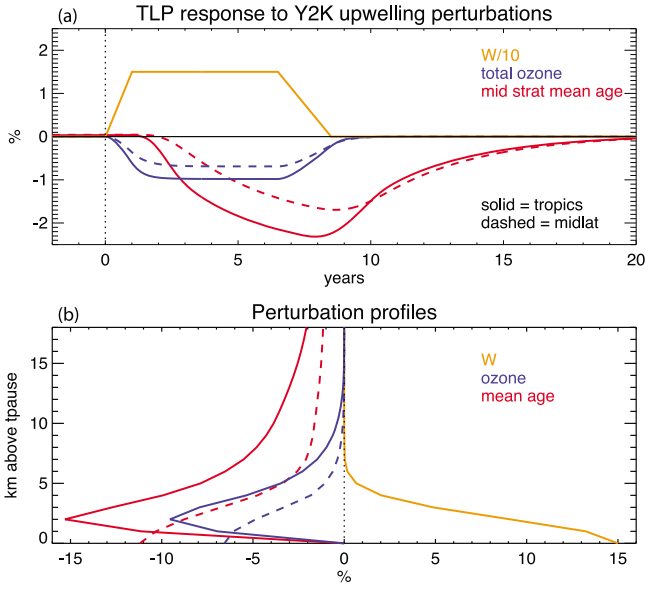

Figure 6. (a) TLP model response to the SST-related vertical velocity and mixing changes following the year 2000. The orange line shows *w* perturbations, scaled by a factor of 10, used as input into the model. The blue and red lines show the total ozone and midstratospheric (average from 15 to 25 km above the tropopause) mean age response, respectively. Year zero in the plot corresponds to the year 2000. (b) Vertical profiles of the input perturbation in *w* (orange line), the tropical and midlatitude ozone responses (blue lines), and the tropical and midlatitude mean age responses (red lines) at year 5 or the year 2005.

between the midlatitudes and tropics associated with the *w* perturbations but we do not show them here.

[29] The ozone and mean age responses in the TLP model have several interesting features. First, the tropical total ozone decreases as expected with a time variation roughly similar to that of the *w* perturbations (Figure 6a) and a peak magnitude of −1%. The profile of tropical ozone changes, shown in Figure 6b 5 years following the initiation of the circulation changes, has a peak ozone decrease a few kilometers above the tropopause and small decreases as high as 10 km above the tropopause. The shape of the tropical ozone changes is similar to that seen in satellite and ozonesonde observations [*Randel et al.*, 2006] and the peak magnitude of −9% is on the same order as the SAGE II ozone anomaly, though smaller than individual ozonesonde anomalies of up to −30%. These differences in magnitude are expected since the model represents an average over 20°S–20°N. The tropical total ozone time series with the TLP ozone perturbations after the year 2000 removed is shown by the green line in Figure 4a. This shows that the SST-related circulation changes can account for most of the tropical total ozone decrease in the early 2000s.

[30] A second interesting feature that does not appear to match the observations is the midlatitude total ozone decrease of just over 0.5%. This is in contrast to the roughly 2% increase in both the Southern Hemisphere and Northern Hemisphere midlatitude TOMS/SBUV total ozone anomalies following the year 2000 (Figure 4b). The decrease in midlatitude total ozone in the model is due to the increased horizontal advection of low ozone mixing ratios out of the tropics in the altitude range of the *w* perturbation with a peak decrease in ozone mixing ratios at the tropopause. The discrepancy between the modeled and observed midlatitude ozone anomalies may be due to details of the mean circulation in the midlatitudes that are not captured in the simple model. In particular, an increase in downward advection acting on the vertical gradient of ozone could overcome the horizontal advection of ozone from the tropics. In a TLP model simulation where the vertical diffusion was large (0.5 m^2/s), the midlatitude total ozone perturbation was positive, in agreement with the observations, due to the increased vertical flux of high ozone into the lower stratosphere.

[31] Another interesting feature is the response of the midstratospheric (average from 15 to 25 km above the tropopause, roughly corresponding to the 30–5 hPa range) mean age of air to the *w* perturbations. Both the tropical and midlatitude mean age decrease by 1.5%–2.5% with larger decreases in the tropics. There is a delay of the mean age response of just over a year in the tropics and nearly 2 years in the midlatitudes, consistent with the time scale for the influence of the near tropopause vertical velocity perturbation to propagate to at least 15 km above the tropopause. Some amount of mean age decrease also persists for over 10 years following the end of the *w* perturbations. This clearly shows the time scale that the effects of the circulation anomalies remain in the stratosphere and is directly related to the length of the tail in the age distribution [e.g., *Waugh and Hall*, 2002].

5.3. Long-Term Trends

[32] The long-term trends in mean age shown in Figure 3 and the "residual" total ozone shown in Figure 4 are assumed to be due to long-term changes in the stratospheric circulation and mixing. For total ozone, the residual trends in the tropics and midlatitudes are both small and positive, 0.16% ± 0.1%/decade in the tropics and 0.25% ± 0.23%/decade and 0.06% ± 0.28%/decade in the northern and southern midlatitudes, respectively, as shown in Table 1. There is clearly still short-term variability left over in each of the residual total ozone time series that has not been removed by the multiple linear regression. But we focus here on the long-term variability of the time series and the circulation changes that may have caused them.

[33] To guide the TLP model long-term trend simulations, we use trends in the residual vertical velocity and horizontal mixing, as represented by the effective diffusivity, estimated from three different reanalyses. The residual vertical velocity was calculated using the TEM definition of $\overline{w}^*$ [*Andrews et al.*, 1987] and a tropical linear trend was computed for the 20°S–20°N average for the JRA-25 and ERA-40 data sets. A residual vertical velocity was not calculated for NCEP since no vertical velocity above 100 hPa is provided with this data set. As mentioned earlier, the stratospheric mean circulations in the reanalysis data sets do not necessarily accurately represent the actual mean circulation. Thus, trends in the reanalysis circulations may not accurately represent actual trends. However, these are the best available data sets for this type of analysis, and we use the trends as examples of what may have occurred.

[34] As shown in Figure 7, both the JRA-25 (solid blue line) and the ERA-40 (dashed blue line) tropical upwelling trends are positive in the lower stratosphere and then become

Table 1. Trends From Observations and TLP Model[a]

	Tropical Total Ozone	Midlatitude Total Ozone	Midstratosphere Midlatitude Mean Age of Air
Observations[b]	0.16 ± 0.1	0.25 ± 0.23 NH 0.06 ± 0.28 SH	4.8 ± 4.5 NH
TLP model with w* trend from JRA, ERA, CCMVal	0.0, −0.3, −0.7	−0.02, 0.06, 0.1	1.0, −0.2, −1.9
TLP model with τ trend from JRA, NCEP	0.15, 0.5	0.03, 0.05	1.6, 4.9
TLP model with w* trends from CCMVal and idealized τ trends	−0.8, −0.1	0.1, 0.1	−2.7, 1.6

[a]Trends in %/decade.
[b]The observed trends of total ozone are the "residual" trends as shown in Figure 4, which are the best estimate of ozone trends due to long-term stratospheric circulation changes.

negative from the middle stratosphere into the lower mesosphere. The ERA-40 trend is substantially more positive in the lower stratosphere and the region of positive trends extends higher into the middle stratosphere compared to JRA-25. The vertical structure of the trends is interesting because the positive trend in the lower stratosphere is consistent with other observational analysis suggesting a strengthened circulation as mentioned in the introduction, but the negative trend in the middle and upper stratosphere is consistent with what would be expected to allow for the observed positive trend in midlatitude mean age to be possible. A similar vertical structure in changes in tropical upwelling covering a shorter period were noted in a study by *Rosenlof* [2002] based on a radiative calculation of the residual circulation using observed temperature and ozone fields. Also included in Figure 7 is the average tropical residual vertical velocity trend profile from seven different CCMVal-2 models (blue dash-dot-dotted line). The CCMVal-2 trend profile has a similar shape to those from the reanalysis data sets but is more strongly positive throughout the lower and middle stratosphere. It should be mentioned that the ERA-40 residual circulation is known to produce unrealistically small mean ages throughout the stratosphere as shown by *Monge-Sanz et al.* [2007] and most CCMs have also had difficulty simulating observed mean ages [e.g., *Eyring et al.*, 2006]. This deficiency in simulating mean age may also be due to errors in mixing, both horizontal and vertical, in the CCMs [e.g., *Hall et al.*, 1999]. We are not aware of any study analyzing mean age of air from the JRA-25 residual circulation. Nevertheless, the trends in the residual vertical velocities from the reanalysis and CCMVal-2 data sets span a range of possibilities that can be investigated in the TLP model.

[35] The trend in the tropical midlatitude mixing time scale τ is more difficult to estimate than the vertical velocity trend because there is no direct means of calculating τ from reanalysis output. We chose to use the effective diffusivity calculated on isentropic surfaces as a diagnostic of horizontal mixing [e.g., *Haynes and Shuckburgh*, 2000]. The edge of the tropical pipe varies as a function of pressure, typically from 20° to 35° latitude. So to encompass mixing across the pipe edge at all levels in the TLP model we averaged the effective diffusivity from 10° to 40° in both hemispheres. We make the assumption that changes in this subtropical average effective diffusivity correspond with changes in the mixing time scale τ. As a sensitivity test, we calculated average effective diffusivity for different subtropical latitude ranges as well as latitude ranges around the time-dependent turnaround latitude in each hemisphere where the TEM residual vertical velocity changes sign (not shown). Averaging around the time-dependent turnaround latitude would account for any trend in the width of the tropical pipe that may affect the trend calculated over a fixed latitude range. There were some small differences in the magnitude of the effective diffusivity trends but the pattern was generally the same among all of the averaging ranges.

[36] The effective diffusivity was calculated on isentropic surfaces from the tropopause up to 700 K, which corresponds to roughly 15 hPa. The reanalyses fields on isentropic surfaces used for the effective diffusivity calculation were obtained from the National Center for Atmospheric Research mass storage system; the vertical resolution varied from 20 to 50 K depending on the isentropic surface and the reanalysis. The profile of the subtropical average effective diffusivity trends in %/decade are shown by the green lines in Figure 7. There is general agreement among the three reanalyses showing a large positive trend in the mixing in the stratosphere. Each of the trend profiles peaks at a slightly different

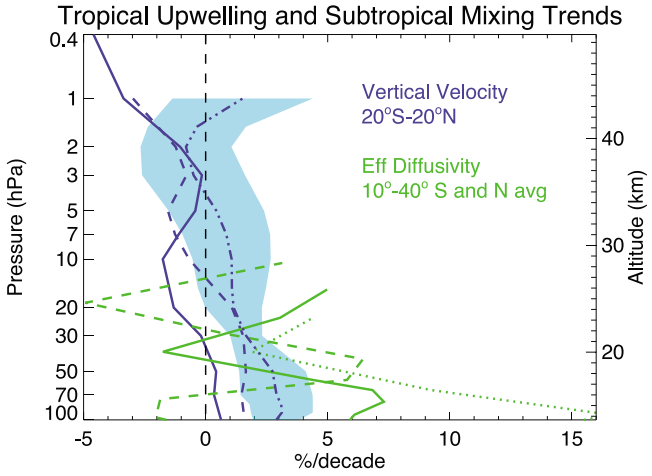

Figure 7. Profiles of tropical vertical velocity and subtropical effective diffusivity trends calculated from the several reanalysis data sets and CCMVal-2 output. The solid lines represent JRA-25 trends, the dashed lines represent ERA-40, the dash-dot-dotted line represents CCMVal-2, and the dotted line represents NCEP. The effective diffusivity trends were calculated from the time series of average effective diffusivity in the 10°–40° latitude range in both Southern Hemisphere and Northern Hemisphere. The light blue shading is the one standard deviation spread of the CCMVal-2 upwelling trends for the nine models included in this study.

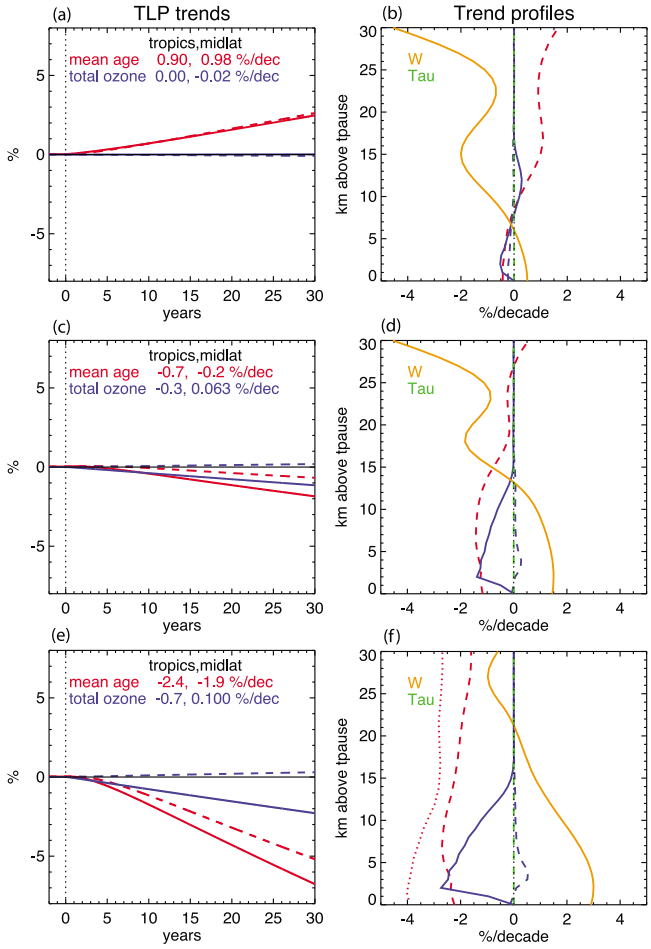

Figure 8. Mean age and ozone trends from the TLP model for three different scenarios of vertical velocity and mixing trends based on the JRA trends shown in Figure 7. The right column (Figures 8b, 8d, and 8f) shows profiles of the tropical vertical velocity (orange line) and mixing (green dashed line) trends input into the model as well as the model output ozone trends in the tropics (blue solid line) and midlatitudes (blue dashed line) and the midlatitude mean age trend (red dashed line). The average 35°N–60°N mean age trend profile from the CCMVal-2 models is shown by the red dotted line in Figure 8f. The left column (Figures 8a, 8c, and 8e) shows time series of the model output total ozone (blue lines) and midlatitude mean age averaged over altitudes 15–25 km above the tropopause (red lines). Solid lines represent the tropics and dashed lines the midlatitudes. Year zero is when the vertical velocity and mixing trends were initiated in the model. The model linear trends for total ozone and 15–25 km mean age for both the tropics and midlatitudes in %/decade are shown for each scenario. The trends shown were calculated in the 20–30 year period following initiation of the vertical velocity and mixing perturbations.

level and with a different magnitude, but all have a double peak structure with one maximum in the lower stratosphere and indications of a secondary maximum in the middle stratosphere, although we cannot resolve the details of the higher peak. The substantial increase in mixing in the subtropical lower stratosphere is likely related to the strengthened circulation in this region due to the connection between wave breaking, which causes horizontal mixing, and the stratospheric mean meridional circulation below the level of breaking. It is not necessarily expected that the mixing and vertical velocity trends would cover the same altitude range since the downward control concept suggests that only momentum deposition due to wave breaking above a given pressure level will contribute to the vertical velocity at that level [*Haynes et al.*, 1991]. However, as shown by *Kerr-Munslow and Norton* [2006], most of the mean vertical velocity variability near the tropical tropopause is driven by wave breaking in a narrow vertical region of the lower stratosphere. The nearly coincident vertical region of subtropical mixing and tropical vertical velocity trends from the JRA-25 data seems to be consistent with *Kerr-Munslow and Norton* [2006] and indicates that an increase in wave breaking in the lower tropical and subtropical stratosphere has been important in driving the strengthening of the lower stratospheric transport circulation.

[37] A number of TLP model simulations were performed with different w and τ trends to investigate the range and sensitivity of total ozone and mean age responses. The values of the mean age and total ozone trends from each of the simulations are shown in Figures 8–10 and also in Table 1 to compare to the observed trends. The trends of mean age produced by the TLP model shown in Table 1 were calculated over the 20–30 year period following the initiation of the perturbations, since there is a lag in the response of the mean age to the circulation perturbations. Thus, although the input w and τ perturbations are linear, the mean age response only approaches a linear shape after roughly 15–20 years at which

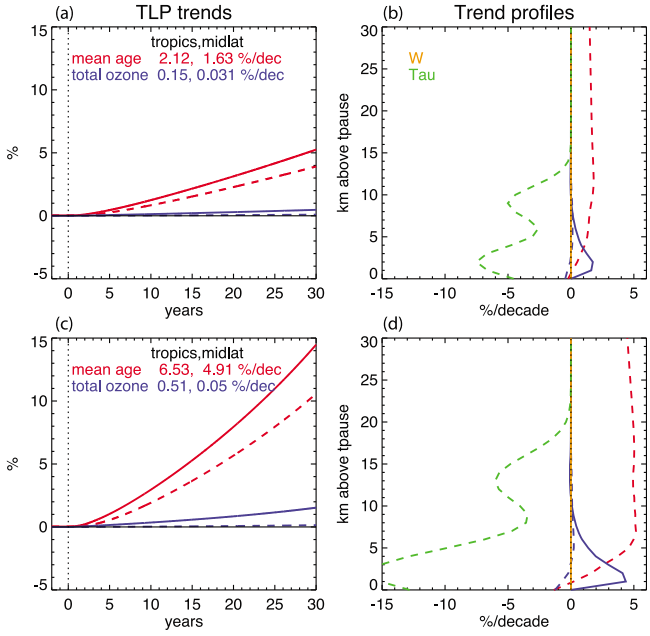

Figure 9. Mean age and ozone trends from the TLP model for two different scenarios of mixing time scale (τ) trends based on the JRA-25 and NCEP trends shown in Figure 7. All of the details of the plots are the same as in Figure 8.

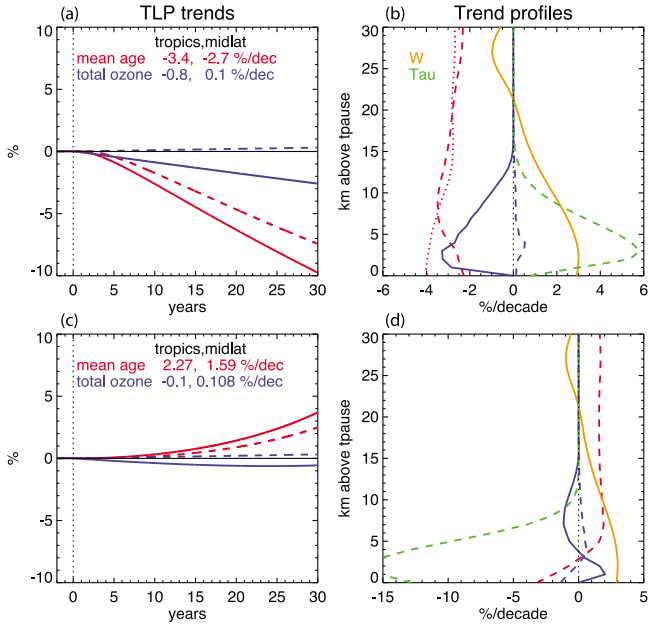

Figure 10. Mean age and ozone trends from the TLP model for two different scenarios of mixing time scale (τ) trends, both use the same vertical velocity trends based on the CCMVal-2 models. All of the details of the plots are the same as in Figure 8. The τ trend profile used in Figures 10a and 10b is an attempt to match the TLP mean age trend with the average Northern Hemisphere midlatitude trend from the CCMVal-2 models shown by the dotted red line. The τ trend profile used in Figures 10c and 10d is similar in shape and magnitude to the trends in the reanalysis data sets. This run shows that increased mixing in the lower stratosphere can offset an increased mean circulation to cause a positive trend in mean age in the midstratosphere.

point the effects of the circulation perturbations have had time to translate throughout the stratosphere and mesosphere and the mean age response begins to approach equilibrium. This, of course, points out a difficulty in interpreting observed mean age variability given what is observed at one particular time is a result of the integrated effect of the variations in mean circulation and mixing over the previous 10–15 years. One consequence of this is that the circulation changes that caused the nearly 30 year observed trend of mean age began a number of years before the first observation was made.

[38] The simulations shown in Figure 8 used smoothed versions of the w trend profiles of JRA-25 (Figures 8a and 8b), ERA-40 (Figures 8c and 8d), and CCMVal-2 (Figures 8e and 8f) as input to the TLP model with no mixing trend. It is clear from Figure 8 that these three w trends have very different impacts on the tropical total ozone and mean age trends. The time series in Figures 8a, 8c, and 8e are the TLP values of total ozone (blue lines) and mean age averaged over 15–25 km above the tropopause (red lines) in the years following the initiation of the perturbation trends in w (year 0). The midlatitude mean age trend from the JRA-25 simulation is smaller than the mean observed trend, although it lies within the uncertainty of the observed trend (Figure 8a). That is in contrast to the midlatitude mean age trends from the ERA-40 and CCMVal-2 simulations that are both negative (Figures 8c and 8e). The increased upwelling in the tropical lower stratosphere in each of the simulations causes a decrease in both tropical ozone mixing ratios and midlatitude mean age in the lower stratosphere. But in the JRA-25 simulation, the decreased upwelling in the tropical midstratosphere and upper stratosphere caused an increase in tropical ozone from roughly 8 to 15 km above the tropopause, above which the chemical time scale of ozone production and loss is too short to be influenced directly by the mean circulation that offsets the lower stratospheric ozone decrease to result in no change in tropical total ozone. The region of decreased tropical upwelling in JRA-25 also resulted in a positive trend in midlatitude mean age above roughly 12 km above the tropopause, which results in the positive mean age trend in Figure 8a.

[39] In the ERA-40 simulation, the altitude of decreased upwelling is higher than that in JRA-25, and although this causes the midlatitude mean age trend to become smaller in the upper stratosphere, it is still negative (Figure 8d). The tropical ozone in the ERA-40 simulation is decreased significantly in the lower stratosphere in response to the increased upwelling, and this causes the negative trend seen in Figure 8c. The CCMVal-2 simulation has the greatest tropical upwelling trend and consequently the largest negative midlatitude mean age and tropical total ozone trends (Figure 8e). Also included in Figure 8f is the 35°N–60°N average mean age trend profile from the CCMVal-2 model REF-B1 runs (dotted red line). Note that the CCMVal-2 mean age trends are more negative at all levels than those from the TLP simulation. Of course, the CCMVal-2 trends included trends in mixing between the midlatitudes and tropics that were not included in this TLP simulation. We will come back to the implications of this discrepancy later in this section.

[40] The midlatitude total ozone trends are small in all of the simulations, roughly in agreement with the observations. In the ERA-40 and CCMVal-2 simulations, the midlatitude ozone increases slightly in the lower stratosphere due to greater downward vertical advection of high-ozone mixing ratios that overcomes the greater horizontal advection of low ozone out from the tropics. The tropical ozone trend profile from the JRA-25 simulation is most similar in shape and magnitude to the residual tropical ozone trend profile from the *Randel and Wu* [2007] data set. The ERA-40 and CCMVal-2 simulations have much larger negative trend values in the lower stratosphere and no region of positive trends above 5 km above the tropopause.

[41] In the second set of simulations shown in Figure 9 trends in the mixing time scale τ based on the JRA-25 and NCEP effective diffusivity trend profiles in Figure 7 were used as input to the TLP model with no trend in w. The ERA-40 case is not shown, since the results are very similar to those from JRA-25. Positive trends in effective diffusivity are represented as negative trends in the mixing time scale τ, since this is consistent with an increase in mixing between the midlatitudes and tropics. The increased mixing in the lower and midstratosphere in both simulations causes positive trends in midlatitude mean age throughout the stratosphere and tropical ozone in the lower stratosphere. The values of the midlatitude mean age trend of 1.6% and 4.9%/decade

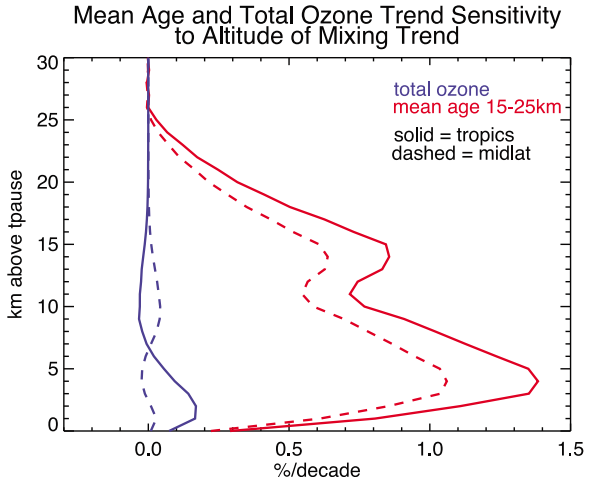

Figure 11. Sensitivity of mean age and total ozone in the TLP model to the altitude of the mixing trend. The value plotted at each level is the total ozone (blue lines) or mean age averaged from 15 to 25 km above the tropopause (red lines) trend due to a 10%/decade decrease in the mixing time scale τ at that level.

(Figures 9a and 9c) are both within the uncertainty of the observed mean age trend and are significantly larger than the positive mean age trend from JRA-25 w changes alone. This clearly demonstrates the importance of trends in mixing between the midlatitudes and tropics in accurately simulating the mean age trends. The tropical total ozone trends are roughly equal to those observed in the JRA-25 mixing case And somewhat larger than observed in the NCEP mixing case. Midlatitude total ozone trends are again quite small as in the simulations with only w trends. The tropical ozone trends in the lower stratosphere are of the opposite sign as those from the *Randel and Wu* [2007] residual ozone trend profiles, and this along with the too large tropical total ozone trends in the NCEP case may suggest an upper limit on the mixing trend.

[42] When trends in both w and τ are used as inputs to the TLP model (not shown), the mean age and total ozone trends are roughly the same as adding together the trends from the individual w and τ simulations shown in Figures 9 and 10 and Table 1. Thus, for the JRA-25 w and τ trend case, the tropical total ozone trend is 0.15%/decade and the midlatitude mean age trend is 2.6%/decade. Both the total ozone and mean age trends are well within the uncertainty of the observed trends. For the ERA-40 case the tropical total ozone trend is −0.15%/decade and the midlatitude mean age trend is 1.4%/year. This tropical ozone trend is of the opposite sign to that observed and the mean age trend is within the observed trend uncertainty. Since we do not have a w trend for NCEP, if we assume an ERA-40 w trend along with the NCEP τ trend then the tropical total ozone (0.2%/decade) and the midlatitude mean age (4.7%/decade) trends are very close to the observed trends. This last case matches the observed total ozone and mean age trends best of the three cases considered here. However, if we also consider the *Randel and Wu* [2007] tropical ozone profile trends, the NCEP mixing trends appear to produce too large positive tropical lower stratospheric ozone trends. With consideration of the tropical ozone profile trends, the JRA-25 case is the closest match to all of the observed trends. In general, it appears that a small strengthening of the mean circulation in the lower stratosphere and a moderate weakening of the mean circulation in the middle and upper stratosphere, combined with a moderate increase in horizontal mixing into the tropics over the last three decades gives the best quantitative match to the observed mean age and ozone trends.

[43] To investigate the CCMVal-2 trends further, we performed two TLP model simulations with the CCMVal-2 w trend profile and two different idealized τ trend profiles. In the first case (Figures 10a and 10b) we used a τ trend profile that gave the best match between the TLP midlatitude mean age trend profile and the 35°N–60°N average mean age trend from the CCMVal-2 models (red dotted line in Figure 10b). As shown in Figure 8f, without a mixing trend, the average midlatitude mean age trend from the CCMVal-2 models was more negative at all levels than that from the TLP model simulation using only the CCMVal-2 w trend as input. To make the TLP model mean age trend more negative, we included a τ trend profile that was positive throughout most of the lower stratosphere to produce less mixing between the tropics and midlatitudes. Less mixing of air between the midlatitudes and tropics means less recirculation of air through the tropical pipe and smaller midlatitude mean ages. The agreement between the mean age trend profiles is good above 8 km, but the TLP model mean age trend is still smaller in the 2–10 km range. It should be noted that the tropical total ozone trend in this case of −0.8%/decade is of opposite sign to the observed "residual" tropical total ozone trend. It is even significantly more negative than the unaltered TOMS/SBUV tropical total ozone trend of −0.17%/decade that is obtained without removing any of the known variability described earlier in this paper.

[44] In the second TLP simulation with CCMVal-2 w trends, we used a τ trend profile roughly similar in magnitude to that from NCEP (Figures 10c and 10d). The purpose of this case is to demonstrate that an increase in mixing can overcome an increase in the mean circulation to produce positive midlatitude mean age trends in the middle and upper stratosphere. Figure 10d shows that the midlatitude mean age trend in this case is negative in the lowest 3 km of the stratosphere but becomes positive at all higher levels. The tropical total ozone trend is still of the opposite sign to that observed but the midlatitude total ozone and mean age trends for this case are both of the same sign as those observed and within the observed uncertainty. This clearly shows the importance of mixing into the tropics and the recirculation of air parcels in the stratosphere in the accurate simulation of mean age, ozone, and likely most other trace gases as well.

[45] In a general sense, we can demonstrate the sensitivity of mean age and total ozone trends to the altitude of mixing trends in the TLP model by performing multiple simulations, each with a 10% decrease in τ peaked at a single altitude. Figure 11 shows the results where the value plotted at each altitude is the trend in either total ozone (blue lines) or mean age averaged from 15 to 25 km above the tropopause (red lines) due to a 10% increase in mixing at that altitude. This plot shows that the middle and upper stratospheric mean age is most sensitive to mixing between the midlatitudes and tropics in the 2–7 km range above the tropopause. This sen-

sitivity to mixing decreases with height up to 25 km above the tropopause. The total ozone is primarily sensitive to mixing in the lowest 10–12 km of the stratosphere.

6. Discussion

[46] What do these results mean as far as CCMs are concerned? It is clear that there is a significant discrepancy between the stratospheric circulation changes simulated by most current CCMs and the changes described in this study that are consistent with the observed mean age of air and total ozone. Only a few studies have analyzed the details, beyond simply an increase in stratospheric wave drag, of what causes the CCMs to produce a strengthening stratospheric circulation. One recent study to do so is of *McLandress and Shepherd* [2009], which analyzed the changes in wave activity in the Canadian Middle Atmosphere Model (CMAM), one of the models that participated in CCMVal-2. They found that 60% of the long-term trend in upward mass flux in the tropical lower stratosphere was due to resolved waves and 40% to parameterized orographic gravity waves. And of the resolved wave trend, 60% was due to planetary waves and 40% to synoptic waves, with most of the synoptic wave contribution occurring in the winter. There was some change in the wave propagation in the stratosphere due to changes in the strength of the subtropical jets, but this was not thought to contribute substantially to the circulation trends. Thus, their conclusion was that trends in waves of all scales, planetary, synoptic, and gravity waves are important in contributing to the stratospheric circulation trends. In another study, tropical upwelling trends in the Whole Atmosphere Community Climate Model 3 (WACCM3) [*Garcia and Randel*, 2008] were found to be due to changes in the propagation and location of wave dissipation. The WACCM3 analysis only divided the wave driving into that due to resolved and parameterized waves, but they found little change in the generation of either type of wave activity. These results are not necessarily in opposition to those from *McLandress and Shepherd* [2009], since each study used different latitudinal averages to diagnose upwelling trends. Also, interestingly, the strengthened circulation in WACCM3 in the lowest part of the stratosphere was mostly due to resolved waves, while the strengthened circulation in the middle and upper stratosphere was entirely due to parameterized gravity waves. In a study of all of the CCMs that took part in CCMVal, *Butchart et al.* [2010] found that an increase in subtropical jet wind speeds and subsequent increase in the altitude at which both resolved waves and parameterized orographic gravity waves break that was a robust result in all of the CCMs. This change in the altitude of wave momentum deposition caused a speed up of the Brewer-Dobson circulation and correlated decrease in mean age throughout the depth of the stratosphere.

[47] Any changes in wave propagation and breaking in the CCMs will also cause changes in the mixing between the midlatitudes and tropics. As shown by *Eyring et al.* [2006], most CCMs have difficulty simulating the correct phase and amplitude of the tropical tape recorder signal in water vapor. The tape recorder signal is greatly affected by mixing into the tropics, and so this indicates that this type of mixing is a large uncertainty in CCMs. Thus, it may be difficult for CCMs to accurately simulate trends in mixing that have been shown here to be important in accurately determining trends in mean age.

[48] From the few studies of trends in CCM wave activity, it is apparent that the strengthening of the stratospheric circulation in response to past and future greenhouse gas changes is a robust result among all models and that both resolved and parameterized waves are important in producing the stratospheric circulation trend. This means that nearly every tropospheric process that produces waves that propagate into the stratosphere is involved, as well as changes in the upper tropospheric and stratospheric zonal mean temperature and wind speed distributions that affect where the waves propagate and dissipate. This change in the characteristics of the wave breaking in the CCMs apparently does not have a significant effect on the amount of mixing between the midlatitudes and tropics since the negative correlation between mean circulation strength and mean age is maintained [e.g., *Butchart et al.*, 2010]. We demonstrate with the TLP model that any increase in mixing from the midlatitudes into the tropics will offset the mean age decreases from a stronger mean circulation either partially or completely, thus decreasing or changing the sign of the correlation between the mean circulation strength and mean age.

7. Summary

[49] In this study, we have used a simple model of the stratosphere, the TLP model, to show possible mean circulation and horizontal mixing variability that can explain the observed variability in both stratospheric mean age and "residual" total ozone over the last three decades. The TLP model was shown to be effective at simulating ozone variability following volcanoes and the lower stratospheric circulation increase in the early 2000s. The volcanic perturbations to the circulation and photochemistry of the stratosphere produce large decreases in lower stratospheric and total ozone in the TLP model in agreement with recent CCM simulations [*Telford et al.*, 2009]. The volcanic perturbations produced no significant change in the mean age in the TLP model due to the small and short (several months) increase in tropical upwelling following each eruption. The large increase in tropical upwelling in the early 2000s caused large changes in both ozone and mean age. Tropical total ozone decreased by nearly 1% in the TLP model in the early 2000s, while midlatitude ozone decreased by roughly 0.5%. The timing and magnitude of the tropical ozone changes are similar to those seen in the TOMS/SBUV total ozone time series. Mean age in both the tropical and midlatitude middle stratosphere was shown to decrease by 1%–2% during the period of tropical upwelling increase in the TLP model, with smaller but still significant mean age decreases persisting for more than 10 years after the end of the upwelling perturbation. This demonstrates the persistence of transient perturbations to the stratospheric circulation.

[50] Using reanalyses trends in TEM residual vertical velocities and subtropical mixing as a guide, the TLP model was able to quantitatively reproduce the observed trends in mean age and total ozone since the late 1970s within uncertainties. The best match in the TLP model to the observed mean age and ozone trends resulted from a small strengthening of the mean circulation in the lower stratosphere and a moderate weakening of the mean circulation in the middle

and upper stratosphere, combined with a moderate increase in horizontal mixing into the tropics. The magnitude of the changes in the mean circulation is uncertain since there is a large uncertainty in how much the mixing into the tropical pipe has changed. We show that it is the changes in the horizontal mixing into the tropics that are most important in quantitatively reproducing the observed trends, in particular, that of mean age in the middle and upper midlatitude stratosphere. A large positive trend in mixing, as suggested by a positive trend in subtropical effective diffusivity in the lower stratosphere in all of the reanalyses considered here, increased both the mean age and tropical total ozone trends substantially. Without the trend in lower stratospheric mixing, the TLP model could not quantitatively match the observed midlatitude mean age trend.

[51] We also used as input to the TLP model the average vertical profile of trends in the mean circulation produced by CCM simulations of the recent climate based on the CCMVal-2 activity. These CCM simulations produce a mean circulation that has strengthened substantially in the lower and middle stratosphere and changed little or slightly weakened in the upper stratosphere depending on the model. The differences in the mean age and tropical total ozone trends from the TLP model using the reanalyses versus CCMVal-2 circulation trend profile as input are substantial, with the CCMVal-2 based trends of opposite sign to those from JRA-25 as well as from the observations. Using the CCMVal-2 mean circulation trends as input, it was also necessary to introduce a trend of decreased mixing in the lower stratosphere, opposite to that suggested by the reanalyses, to most closely match the TLP midlatitude mean age trend to that calculated from the average 35°N–60°N mean ages from the CCMs.

[52] Of course, the TLP model is highly simplified, and so we do not expect a quantitative match between the simulated and observed variability in mean age and total ozone. In particular, the TLP model does not represent the polar regions, which are most likely to affect the midlatitude ozone and mean age. Also, with regard to the observations used in this study, there are clearly significant uncertainties associated with the trends in midlatitude mean age and the "residual" total ozone. The uncertainties in the mean age trend come from both the measurements themselves and the technique used to calculate the mean age as described in section 2. For total ozone, the calculation of "residual" trends involves the removal of variability due to a variety of cycles and trends that are not perfectly known. However, even with the limitations of the TLP model and the observations, the general results described above should be robust. That is, the relationship between the mean age and total ozone responses to circulation and mixing changes, the suggestion of a recent slowing trend of the mean circulation in the middle and upper stratosphere and an increase in mixing between the midlatitudes and tropics in the lower stratosphere, and the importance of mixing in the lower stratosphere to the quantification of mean age changes.

[53] The stratospheric mean age of air data set produced by *Engel et al.* [2009], even with the large uncertainties associated with it, is the best available observationally based indicator of stratospheric circulation changes over the last three decades. There are other stratospheric observational data sets that span this time period, including radiosondes [e.g., *Randel et al.*, 2009], frost point water vapor balloon measurements from Boulder [*Scherer et al.*, 2008], microwave sounding unit and stratospheric sounding unit temperatures (e.g., P. J. Young et al., Changes in stratospheric temperatures and their implications for changes in the Brewer-Dobson circulation. 1979–2005, submitted to *Journal of Climate*, 2010), and the TOMS/SBUV total ozone data set used in this study, which are all important to consider when investigating stratospheric circulation changes. But only the mean age data set is entirely determined by the stratospheric mean meridional circulation and mixing between the midlatitudes and tropics. Hopefully, more long-term observations that tell us about the stratospheric circulation will become available in the coming years. Until then, we need to more fully understand the limited number of observational data sets that tell us about the past three decades of stratospheric circulation and mixing changes. This further understanding is necessary so we can be more confident in the predictions of future changes.

[54] **Acknowledgments.** This work was supported by the NOAA ACCP program. We appreciate the public availability of the JRA-25 output (obtained from http://dss.ucar.edu/data sets/ds625.0/) and the NCEP/NCAR Reanalysis (obtained from the NOAA ESRL Physical Sciences Division, http://www.cdc.noaa.gov). The ERA-40 data for this study are from the Research Data Archive (RDA), which is maintained by the Computational and Information Systems Laboratory (CISL) at the National Center for Atmospheric Research (NCAR). NCAR is sponsored by the National Science Foundation (NSF). The original ERA-40 data are available from the RDA (http://dss.ucar.edu) in data set ds117.3. The contributions of Neal Butchart and Steven Hardiman were support by the Joint DECC and Defra Integrated Climate Programme, DECC/Defra (GA01101). We also thank Emily Shuckburgh for providing the code to calculate effective diffusivity.

References

Andrews, D. G., J. R. Holton, and C. B. Leovy (1987), *Middle Atmosphere Dynamics*, 498 pp., Academic, San Diego, Calif.

Austin, J., and F. Li (2006), On the relationship between the strength of the Brewer-Dobson circulation and the age of stratospheric air, *Geophys. Res. Lett.*, *33*, L17807, doi:10.1029/2006GL026867.

Bacmeister, J. T., D. E. Siskind, M. E. Summers, and S. D. Eckermann (1998), Age of air in a zonally averaged two-dimensional model, *J. Geophys. Res.*, *103*(D10), 11,263–11,288, doi:10.1029/98JD00277.

Butchart, N., et al. (2006), Simulations of anthropogenic change in the strength of the Brewer-Dobson circulation, *Clim. Dyn.*, *27*, 727–741.

Butchart, N., et al. (2010), Chemistry-climate model simulations of 21st century stratospheric climate and circulation changes, *J. Clim.*, *23*, doi:10.1175/2010JCLI3404.1.

Deshler, T., et al. (2006), Trends in the nonvolcanic component of stratospheric aerosol over the period 1971–2004, *J. Geophys. Res.*, *111*, D01201, doi:10.1029/2005JD006089.

Engel, A., et al. (2009), Age of stratospheric air unchanged within uncertainties over the past 30 years, *Nat. Geosci.*, *2*, doi:10.1038/ngeo388.

Eyring, V., T. G. Shepherd, and D. W. Waugh (Eds.) (2010), SPARC CCMVal, SPARC CCMVal Report on the Evaluation of Chemistry Climate Models, SPARC Report No. 5, WCRP-X, WMO/TD-No. X. (Available at http://www.atmosp.physics.utoronto.ca/SPARC)

Eyring, V., et al. (2006), Assessment of temperature, trace species, and ozone in chemistry climate model simulations of the recent past, *J. Geophys. Res.*, *111*, D22308, doi:10.1029/2006JD007327.

Fleming, E. L., C. H. Jackman, D. K. Weisenstein, and M. K. W. Ko (2007), The impact of interannual variability on multidecadal total ozone simulations, *J. Geophys. Res.*, *112*, D10310, doi:10.1029/2006JD007953.

Garcia, R. R., and W. J. Randel (2008), Acceleration of the Brewer-Dobson circulation due to increases in greenhouse gases, *J. Atmos. Sci.*, *65*, 2731–2739.

Garcia, R. R., D. R. Marsh, D. E. Kinnison, B. A. Boville, and F. Sassi (2007), Simulation of secular trends in the middle atmosphere, 1950–2003, *J. Geophys. Res.*, *112*, D09301, doi:10.1029/2006JD007485.

Hadjinicolaou, P., A. Jrrar, J. A. Pyle, and L. Bishop (2002), The dynamically driven long-term trend in stratospheric ozone over northern middle latitudes, *Q. J. R. Meteorol. Soc.*, *128*, 1393–1412.

Hall, T. M., and D. W. Waugh (2000), Stratospheric residence time and its relationship to mean age, *J. Geophys. Res.*, *105*(D5), 6773–6782, doi:10.1029/1999JD901096.

Hall, T. M., D. W. Waugh, K. A. Boering, and R. A. Plumb (1999), Evaluation of transport in stratospheric models, *J. Geophys. Res.*, *104*(D15), 18,815–18,839, doi:10.1029/1999JD900226.

Haynes, P., and E. Shuckburgh (2000), Effective diffusivity as a diagnostic of atmospheric transport 1. Stratosphere, *J. Geophys. Res.*, *105*(D18), 22,777–22,794.

Haynes, P. H., C. J. Marks, M. E. McIntyre, T. G. Shepherd, and K. P. Shine (1991), On the "downward control" of extratropical diabatic circulations by eddy-induced zonal mean forces, *J. Atmos. Sci.*, *48*, 651–678.

Hood, L. L., and B. E. Soukharev (2005), Interannual variations of total ozone at northern midlatitudes correlated with stratospheric EP flux and potential vorticity, *J. Atmos. Sci.*, *62*, 3724–3740.

Kalnay, E., et al. (1996), The NCEP/NCAR 40-year reanalysis project, *Bull. Am. Meteorol. Soc.*, *77*, 437–471.

Kerr-Munslow, A. M., and W. A. Norton (2006), Tropical wave driving of the annual cycle in tropical tropopause temperatures: Part I. ECMWF analyses, *J. Atmos. Sci.*, *63*, 1410–1419.

Konopka, P., J.-U. Grooβ, F. Plöger, and R. Müller (2009), Annual cycle of horizontal in-mixing into the lower tropical stratosphere, *J. Geophys. Res.*, *114*, D19111, doi:10.1029/2009JD011955.

Lamarque, J.-F., D. E. Kinnison, P. G. Hess, and F. M. Vitt (2008), Simulated lower stratospheric trends between 1970 and 2005: Identifying the role of climate and composition changes, *J. Geophys. Res.*, *113*, D12301, doi:10.1029/2007JD009277.

Lee, H., and A. K. Smith (2003), Simulation of the combined effects of solar cycle, quasi-biennial oscillation, and volcanic forcing on stratospheric ozone changes in recent decades, *J. Geophys. Res.*, *108*(D2), 4049, doi:10.1029/2001JD001503.

Legras, B., B. Joseph, and F. Lefevre (2003), Vertical diffusivity in the lower stratosphere from Lagrangian back trajectory reconstructions of ozone profiles, *J. Geophys. Res.*, *108*(D18), 4562, doi:10.1029/2002JD003045.

Li, F., J. Austin, and J. Wilson (2008), The strength of the Brewer-Dobson circulation in a changing climate: Coupled chemistry climate model simulations, *J. Clim.*, *21*, 40–57.

Marsh, D. R., and R. R. Garcia (2007), Attribution of decadal variability in lower-stratospheric tropical ozone, *Geophys. Res. Lett.*, *34*, L21807, doi:10.1029/2007GL030935.

McCormick, M. P., J. M. Zawodny, R. E. Veiga, J. C. Larsen, and P. H. Wang (1989), An overview of SAGE I and II ozone measurements, *Planet. Space Sci.*, *37*, 1567–1586.

McLandress, C., and T. G. Shepherd (2009), Simulated antropogenic changes in the Brewer-Dobson circulation, including its extension to high latitudes, *J. Clim.*, *22*, 1516, doi:10.1175/2008JCLI2679.1.

Mears, C. A., and F. J. Wentz (2009), Construction of the remote sensing systems V3.2 atmospheric temperature records from the MSU and AMSU microwave sounders, *J. Atmos. Ocean Tech.*, *26*, 1040–1056.

Monge-Sanz, B. M., M. P. Chipperfield, A. J. Simmons, and S. M. Uppala (2007), Mean age of air and transport in a CTM: Comparison of different ECMWF analyses, *Geophys. Res. Lett.*, *34*, L04801, doi:10.1029/2006GL028515.

Morgenstern, O., et al. (2010), Review of the formulation of present-generation stratospheric chemistry-climate models and associated external forcings, *J. Geophys. Res.*, *115*, D00M02, doi:10.1029/2009JD013728.

Mote, P. W., T. J. Dunkerton, M. E. McIntyre, E. A. Ray, P. H. Haynes, and J. M. Russell III (1998), Vertical velocity, vertical diffusion, and dilution by midlatitude air in the tropical lower stratosphere, *J. Geophys. Res.*, *103*, 8651–8666.

Neu, J. L., and R. A. Plumb (1999), Age of air in a "leaky pipe" model of stratospheric transport, *J. Geophys. Res.*, *104*(D16), 19,243–19,255, doi:10.1029/1999JD900251.

Newman, P. A., J. S. Daniel, D. W. Waugh, and E. R. Nash (2007), A new formulation of equivalent effective stratospheric chlorine (EESC), *Atmos. Chem. Phys.*, *7*, 4537–4552.

Oman, L., D. W. Waugh, S. Pawson, R. S. Stolarski, and P. A. Newman (2009), On the influence of anthropogenic forcings on changes in the stratospheric mean age, *J. Geophys. Res.*, *114*, D03105, doi:10.1029/2008JD010378.

Onogi, K., et al. (2007), The JRA-25 Reanalysis, *J. Meteorol. Soc. Jpn.*, *85*, 369–432.

Plumb, R. A. (1996), A "tropical pipe" model of stratospheric transport, *J. Geophys. Res.*, *101*(D2), 3957–3972, doi:10.1029/95JD03002.

Portmann, R. W., et al. (1999), Role of nitrogen oxides in the stratosphere: A reevaluation based on laboratory studies, *Geophys. Res. Lett.*, *26*(15), 2387–2390.

Randel, W. J., and J. B. Cobb (1994), Coherent variations of monthly mean total ozone and lower stratospheric temperatures, *J. Geophys. Res.*, *99*(D3), 5433–5447, doi:10.1029/93JD03454.

Randel, W. J., and F. Wu (2007), A stratospheric ozone profile data set for 1979–2005: Variability, trends, and comparisons with column ozone data, *J. Geophys. Res.*, *112*, D06313, doi:10.1029/2006JD007339.

Randel, W. J., F. Wu, H. Voemel, G. E. Nedoluha, and P. Forster (2006), Decreases in stratospheric water vapor after 2001: Links to changes in the tropical tropopause and the Brewer-Dobson circulation, *J. Geophys. Res.*, *111*, D12312, doi:10.1029/2005JD006744.

Randel, W. J., et al. (2009), An update of observed stratospheric temperature trends, *J. Geophys. Res.*, *114*, D02107, doi:10.1029/2008JD010421.

Rosenfield, J. E., D. B. Considine, P. E. Meade, J. T. Bacmeister, C. H. Jackman, and M. R. Schoeberl (1997), Stratospheric effects of Mount Pinatubo aerosol studied with a coupled two-dimensional model, *J. Geophys. Res.*, *102*(D3), 3649–3670, doi:10.1029/96JD03820.

Rosenlof, K. H. (1995), The seasonal cycle of the residual mean meridional circulation in the stratosphere, *J. Geophys. Res.*, *100*(D3), 5173–5191, doi:10.1029/94JD03122.

Rosenlof, K. H. (2002), Transport changes inferred from HALOE water and methane measurements, *J. Meteorol. Soc. Jpn.*, *80*, 831–848.

Rosenlof, K. H., and G. C. Reid (2008), Trends in the temperature and water vapor content of the tropical lower stratosphere: Sea surface connection, *J. Geophys. Res.*, *113*, D06107, doi:10.1029/2007JD009109.

Scherer, M., H. Vomel, S. Fueglistaler, S. J. Oltmans, and J. Staehelin (2008), Trends and variability of midlatitude stratospheric water vapor deduced from the reevaluated Boulder balloon series and HALOE, *Atmos. Chem. Phys.*, *8*, 1391–1401.

Seidel, D. J., R. J. Ross, J. K. Angell, and G. C. Reid (2001), Climatological characteristics of the tropical tropopause as revealed by radiosondes, *J. Geophys. Res.*, *106*(D8), 7857–7878.

Shepherd, T. G., and A. I. Jonsson (2008), On the attribution of stratospheric ozone and temperature changes to changes in ozone-depleting substances and well-mixed greenhouse gases, *Atmos. Chem. Phys.*, *8*, 1435–1444.

Shine, K. P., et al. (2003), A comparison of model-simulated trends in stratospheric temperatures, *Q. J. R. Meteorol. Soc.*, *129*, 1565–1588.

Solomon, S., R. W. Portmann, R. R. Garcia, L. W. Thomason, L. R. Poole, and M. P. McCormick (1996), The role of aerosol variations in anthropogenic ozone depletion at northern midlatitudes, *J. Geophys. Res.*, *101*(D3), 6713–6727, doi:10.1029/95JD03353.

Solomon, S., K. Rosenlof, R. Portmann, J. Daniel, S. Davis, T. Sanford, and G.-K. Plattner (2010), Contributions of stratospheric water vapor to decadal changes in the rate of global warming, *Science*, doi:10.1126/science.1182488.

Sparling, L. C., J. A. Kettleborough, P. H. Haynes, M. E. McIntyre, J. E. Rosenfield, M. R. Schoeberl, and P. A. Newman (1997), Diabatic cross-isentropic dispersion in the lower stratosphere, *J. Geophys. Res.*, *102*(D22), 25,817–25,829, doi:10.1029/97JD01968.

Stolarski, R. S., and S. M. Frith (2006), Evidence of trend slow-down in the long-term TOMS/SBUV total ozone data record: The importance of instrument drift uncertainty, *Atmos. Chem. Phys.*, *6*, 4057–4065.

Stolarski, R. S., A. R. Douglass, S. Steenrod, and S. Pawson (2006), Trends in stratospheric ozone: Lessons learned from a 3D chemical transport model, *J. Atmos. Sci.*, *63*, 1028–1041.

Strahan, S. E., M. R. Schoeberl, and S. Steenrod (2009), The impact of tropical recirculation on polar composition, *Atmos. Chem. Phys.*, *9*, 2471–2480.

Telford, P., P. Braesicke, O. Morgenstern, and J. Pyle (2009), Reassessment of causes of ozone column variability following the eruption of Mount Pinatubo using a nudged CCM, *Atmos. Chem. Phys.*, *9*, 4251–4260.

Thompson, D. W. J., and S. Solomon (2009), Understanding recent stratospheric climate change, *J. Clim.*, *22*, 1934–1943.

Tie, X. X., G. P. Brasseur, B. Briegleb, and C. Granier (1994), Two-dimensional simulation of Pinatubo aerosol and its effect on stratospheric ozone, *J. Geophys. Res.*, *99*(D10), 20,545–20,562, doi:10.1029/94JD01488.

Uppala, S. M., et al. (2005), The ERA-40 reanalysis, *Q. J. R. Meteorol. Soc.*, *131*(612), 2961–3012.

Volk, C. M., et al. (1996), Quantifying transport between the tropical and midlatitude lower stratosphere, *Science*, *272*, 1763–1768.

Volk, C. M., F. L. Moore, J. W. Elkins, E. A. Ray, G. S. Dutton, D. W. Fahey, J. J. Margitan, and R. J. Salawitch (2000), Ascent and entrainment rates in the tropical stratosphere from balloon-borne in situ observations, 2nd SPARC General Assembly, Mar del Plata, Argentina.

Waugh, D. (2009), The age of stratospheric air, *Nat. Geosci.*, *2*, 14–15.
Waugh, D. W., and T. M. Hall (2002), Age of stratospheric air: Theory, observations and models, *Rev. Geophys.*, *40*(10), 1010, doi:10.1029/2000RG000101.

H. Boenisch, Institute for Atmospheric and Environmental Sciences, Goethe Universität Frankfurt, 60438 Frankfurt, Germany.
P. Braesicke, National Centre for Atmospheric Science Climate-Chemistry Centre for Atmospheric Science, University of Cambridge, Cambridge, CB2 1EW, UK.
N. Butchart and S. Hardiman, Met Office Hadley Centre, Exeter, Devon, EX1 3PB, UK.
S. M. Davis, F. L. Moore, E. A. Ray, and K. H. Rosenlof, Chemical Sciences Division, Earth Systems Research Laboratory, NOAA, 325 Broadway, Boulder, CO 80305, USA. (eric.ray@noaa.gov)
M. Hegglin, Department of Physics, University of Toronto, Toronto, Canada, M5S 1A7.
F. Li, Goddard Earth Sciences and Technology Center, University of Maryland Baltimore County, Baltimore, MD 21228, USA.
E. Mancini and G. Pitari, University of L'Aquila, 67100 Cappito, L'Aquila, Italy.
D. A. Plummer, Canadian Centre for Climate Modelling and Analysis, Environment Canada, Gatineau, Québec, Canada, K1A OH3.
E. Rozanov, Physical-Meteorological Observatory/World Radiation Centre, 7260 Davos, Dorf, Switzerland.
K. Shibata, Meteorological Research Institute, Tsukuba-city, Ibaraki 502-0052, Japan.
D. Smale and O. Morgenstern, National Institute of Water and Atmospheric Research Ltd., Central Otago, Private Bag 50061, Omakau, New Zealand.